Improved Physical Layer Implementation of a MIL-STD-188 CPM Modem

fred harris (fred.harris@sdsu.edu)[1], Richard Bell (richbell@spawar.navy.mil)[2],
[1]San Diego State University, San Diego, CA, USA
[2]Space and Naval Warfare Systems Center Pacific (SSC Pacific)

ABSTRACT

Continuous Phase Modulation (CPM) maintains a constant amplitude and exhibits reasonable spectral confinement. Modern implementations perform direct phase modulation of Direct Digital Synthesizers. The direct phase modulation is understood to be a non-linear modulation process [1]. In spite of this fact most receiver structures demodulate the CPM signal by treating it as an O-QPSK signal. For small phase modulation indices, the errors are small but are not zero. We examine and present CPM receiver structures that perform phase demodulation with time reversed and conjugate phase matched filter aligned with the phase profiles of the modulation processes. We also examine innovative processing techniques that extract Doppler offsets, and perform carrier phase recovery and symbol timing recovery from traditional structured preambles.

I. INTRODUCTION

The digital modulation process alters selected parameters of a sinewave in response to states of a finite state machine. We assign values selected from a limited set of amplitudes, frequencies or phases of a sinewave carrier to form an amplitude shift keying (ASK), a frequency shift keying (FSK) and a phase shift keying (PSK) modulation signal. Specifically, we examine 4-PSK (QPSK, quadrature phase shift keying) and identify 4 equally spaced constellation points on a circle corresponding to the 4 phases. Figure 1 shows the 4-constellation points for a QPSK, two O-QPSK, and a CPM modulator. The signal levels have been scaled for the constellation points to reside on the corners of the unit square which scales the circumscribed circle radius to sqrt(2). The phases can be identified by their polar coordinates as well as by their Cartesian coordinates. Traditionally receivers are designed to determine the Cartesian coordinates of successive symbols by processing and extracting their in-phase and quadrature components. In ordinary QPSK modulation, transitions between constellation points are not specifically controlled but are affected by shaping filters which restrict the modulation bandwidth of the process. The unrestricted transitions result in incidental amplitude modulation. There are a number of reasons to restrict or to control

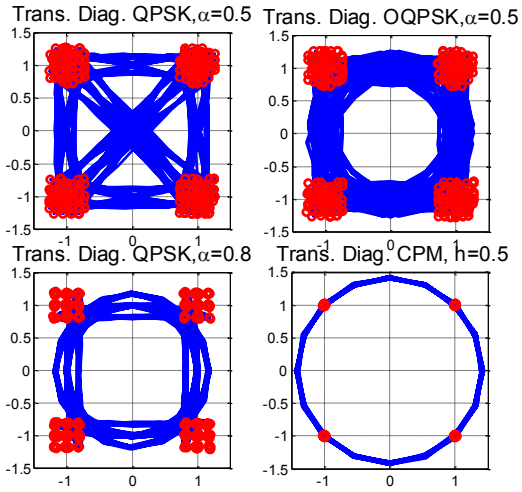

Fig. 1 Constellations and State Transition Profiles for SQRT Nyquist filtered QPSK α=0.5, O-QPSK for α=0.5, and O-QPSK for α=0.8, and CPM Half Sinewave Shaping Filter with Mod. Index h=0.25.

the state trajectories transitioning between states. A common desired attribute avoids trajectories that go through the origin, (to avoid zero amplitude envelope) while another avoids trajectories between repeated states (to ensure state transitions for the synchronizers). One way to avoid trajectories through the origin is to offset the in-phase and quadrature signal components so they cannot simultaneously change states. This modification, called Offset-QPSK (O-QPSK), results in state trajectories that do not transition through the origin but also exhibit reduced amplitude variations. Receivers designed to demodulate O-QPSK are variations of the QPSK modems that accommodate the time offset between the In-Phase and Quadrature signal paths [2]. There is a reason to further control the state transitions between states so that the trajectories between states do not leave the unit circle. We can incorporate this constraint by selecting the shaping filters for the In-Phase and Quadrature components of the O-QPSK to be half sine-waves. An equivalent option is to phase modulate the signal with linear phase profiles in each symbol interval. The constant amplitude envelope permits the final stage power amplifiers in the transmitter to operate at the edge of saturation and thus exhibit maximum power efficiency while preserving signal and spectral fidelity by avoiding non-linear distortion of the output amplifier stage. The half cycle offset sinewave shaping

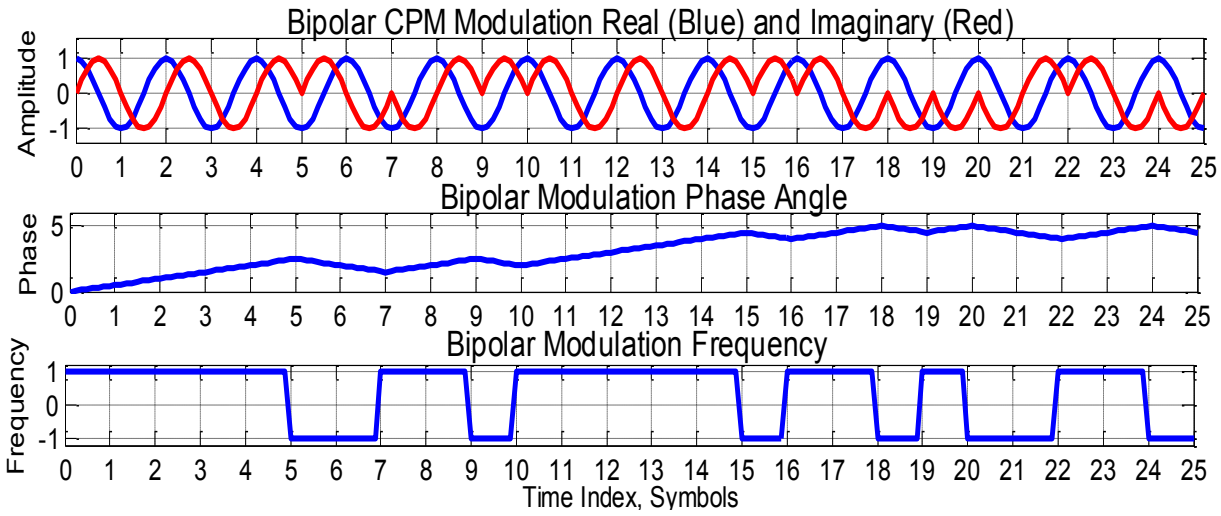

Fig. 2. In-Phase and Quadrature Components of CPM O-QPSK Signal Along with Its Phase and Frequency Profiles.

filter forms a signal with phase continuity across symbol boundaries. The class of signal so formed are described as CPM modulation. An example of the I-Q components of a binary CPM signal is shown in Fig. 2 which also shows its baseband phase and frequency profiles.

Because the CPM signal arrived at its final configuration by transitioning from QPSK through the O-QPSK process we persist in thinking of the CPM signal as an O-QPSK signal. In a true CPM modem the phase is directly modulated and the in-phase and quadrature components of the modulator are correlated. The O-QPSK receiver does not use this correlation while a true phase modulator and demodulator would. We might ask "Why is this a problem?" The answer is, other CPM signals formed by direct modulation of the phase function, such as is done in GSM, the Gaussian filtered Minimum phase Shift Keying (GMSK), is not optimally demodulated by an O-QPSK receiver [3]. In a phase modulated system phase noise and amplitude noise are orthogonal. In an O-QPSK modem, the in-phase and quadrature phase are projected on the two quadrature components and the receiver is unaware that the two signal components are correlated.

Since phase modulation requires a phase reference we find that phase progression due to a frequency error has a severe effect on the demodulation process. Frequency offsets due to Doppler shifts must be removed for successful demodulation. This is true in both the O-QPSK and the true phase demodulator. In the modulation forms described in MIL-STD 188 preambles are used to resolve Doppler frequency offsets and timing clock alignment prior to payload processing. The standard proposes a discrete Fourier transform based technique to resolve Doppler offsets that the standard suggests to be required when the offset is greater than the modulation bandwidth. The standard also references papers supporting the suggested technique [4].

In this paper we present a new technique to extract the Doppler offset information from the preamble which differs significantly from the technique proposed in the standard. We also introduce a demodulation scheme that performs phase matched filtering using the conjugate phase profile of the modulation process and introduce maximum likelihood timing recovery and frequency tracking methods to phase demodulate the CPM signal [5].

II. PREAMBLE PROCESSING

A common preamble for a number of CPM signals is a sequence of repeated phase shifts corresponding to 1 1 0 0 for phase shifts with modulation index 0.5. The waveform formed by this phase profile is one cycle of a complex sinewave corresponding to phasor rotation in the positive direction followed by one complex cycle of a complex sinewave corresponding to phasor rotation in the positive direction followed by one complex cycle of a sinewave with phasor rotation in the negative direction. Fig. 3 shows the Doppler free time series of the preamble along with the preamble distorted by a 9-kHz Doppler shift and then the spectrum of the Doppler shifted preamble. The suggested method of determining the Doppler offset is centered about examination of the preamble's Discrete Fourier Transform (DFT).

An alternate method of determining the Doppler offset frequency is illustrated in Fig. 4. We note that the tones in successive Doppler free preamble intervals are conjugates with frequencies $-\theta_P$ and $+\theta_P$ radians per sample respectively. We then see that when Doppler shifted, the tones in successive intervals are distorted and have new frequencies $+\theta_D-\theta_P$ and $+\theta_D+\theta_P$. The product of the distorted tones from the two intervals forms a third non-distorted tone with frequency $+2\theta_D$.

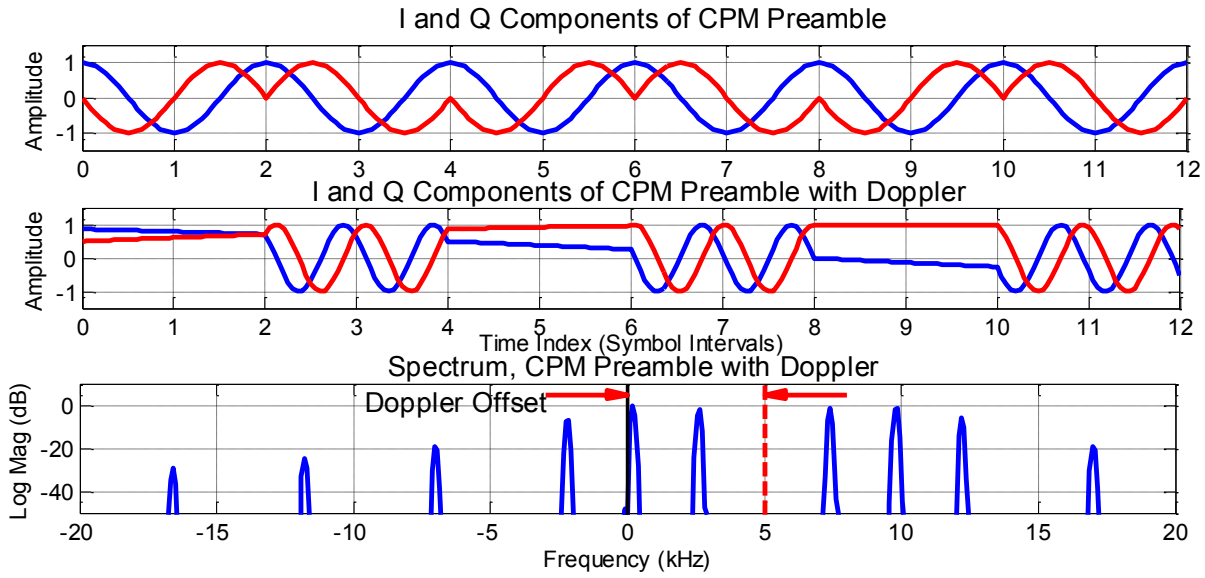

Figure 3. Preamble Pattern Multiple Repetitions of 1 1 0 0, (One Cycle Cos–j Sin & One Cycle (Cos + j Sin) With no Doppler, Same with 5 kHz of Doppler and Spectrum of Dopplered Periodic Preamble Signal.

$$s(\mathrm{n}) = \mathrm{e}^{j\theta_{prmbl}n}\,\mathrm{e}^{j\theta_{dplr}n} : \mathrm{n} = 0:39$$

$$s(\mathrm{n}+40) = \mathrm{e}^{-j\theta_{prmbl}n}\,\mathrm{e}^{j\theta_{dplr}n} : \mathrm{n} = 0:39$$

$$p(n) = s(n)\cdot s(n+40) \qquad (1)$$

$$= \mathrm{e}^{+j\theta_{prmbl}n}\,\mathrm{e}^{j\theta_{dplr}n}\,\mathrm{e}^{-j\theta_{prmbl}n}\,\mathrm{e}^{j\theta_{dplr}n}$$

$$= \mathrm{e}^{\mathrm{j}2\theta_{dplr}n}$$

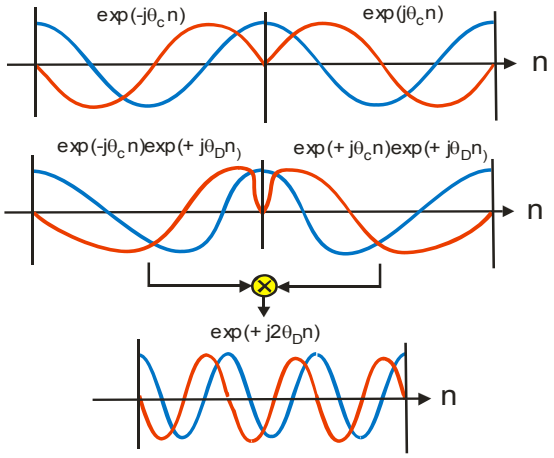

Figure 4. Top Subplot, Doppler Free 4-Symbols of Preamble, Center Subplot, and Same Symbols Doppler Distorted. Bottom Subplot Product of Successive Intervals with Canceled Preamble Modulation Components.

This relationship is shown in eq(1). Figure 5 illustrates formation of the double frequency Doppler tone $+2\theta_D$ formed by the product of the preamble adjacent delayed intervals as well the spectrum of the complex tone formed by that product. The frequency of Doppler tone is obtained from the ATAN of the average conjugate product of successive complex samples of this tone. The Doppler offset can be removed by a complex down conversion formed by a DDS set to the half frequency of the measured tone. This removal process is simple to implement and performs its task remarkably well.

In a similar fashion of delayed product, the conjugate delayed product spanning 4-symbol durations (80 samples) correlates the current sample values with the previous 80 offset samples. Since the data repeats in 4-symbol duration with or without the Doppler offset, the running average of this product forms the cross correlation, which when normalized by the delayed auto correlation forms a very effective squelch signal detector as well as the signal strength estimate to operate an AGC loop. Figure 6 shows the auto and cross product terms, the correlation running average of the two terms, and the normalized correlation ratio of the two averages which crosses the threshold and declares signal present within a few samples of signal start.

For completeness Figure 7 shows the spectrum of the CPM periodic preamble and for the modulated random data. In each figure we overlaid the spectrum of the half sinewave shaping filter and a box indicating the CPM symbol rate of 9.6 kHz. Note the preamble fundamental frequency is 2.4 kHz and the tone in the random modulation is at 4.8 kHz.

-

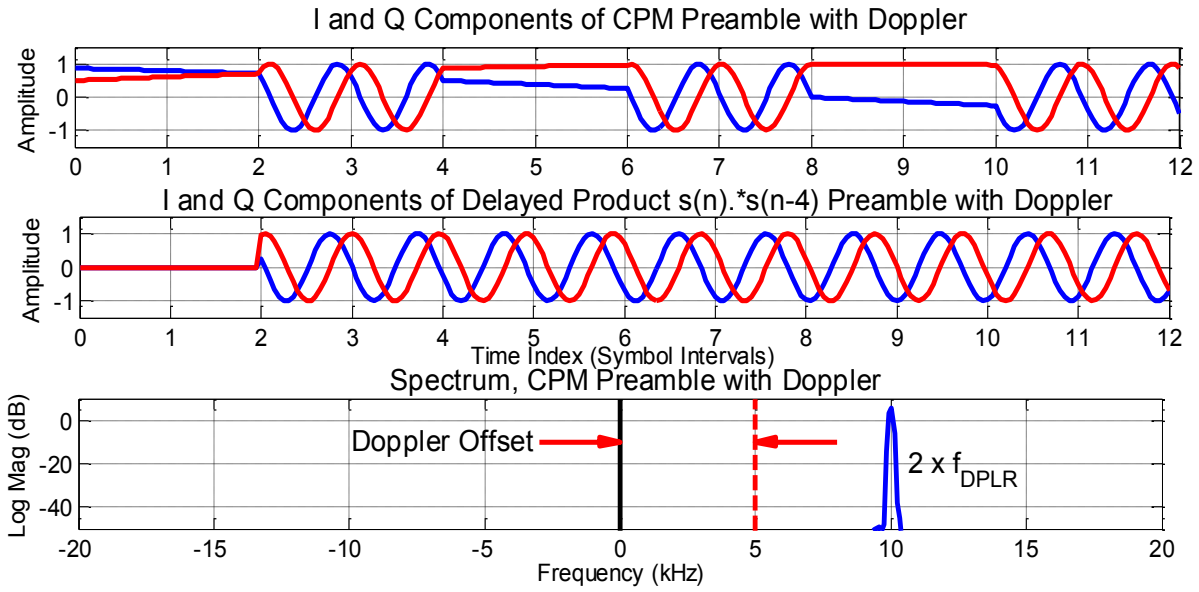

Figure 5. Top Subplot. Doppler Distorted Tones in Successive Preamble Intervals Center Subplot, Product of Successive Conjugate Symbol Intervals Forms Complex Tone at Twice Doppler Frequency. Third Subplot Spectrum of Doppler Tone Formed.

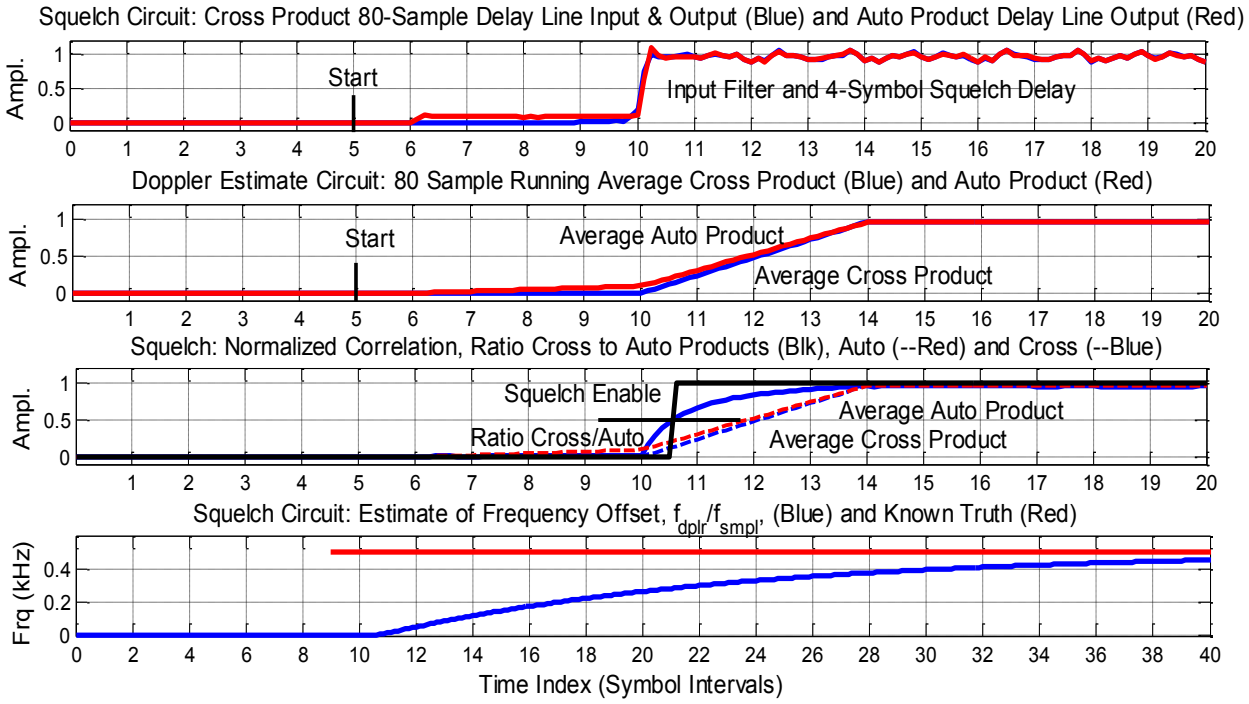

Figure 6. Squelch Network, Auto and 4-Symbol Delayed Conjugate Cross Product and Auto and Cross Correlation Normalized Correlation and Threshold Crossing, 2-Symbol Delayed Product, and 0.3 kHz Doppler Frequency Estimate.

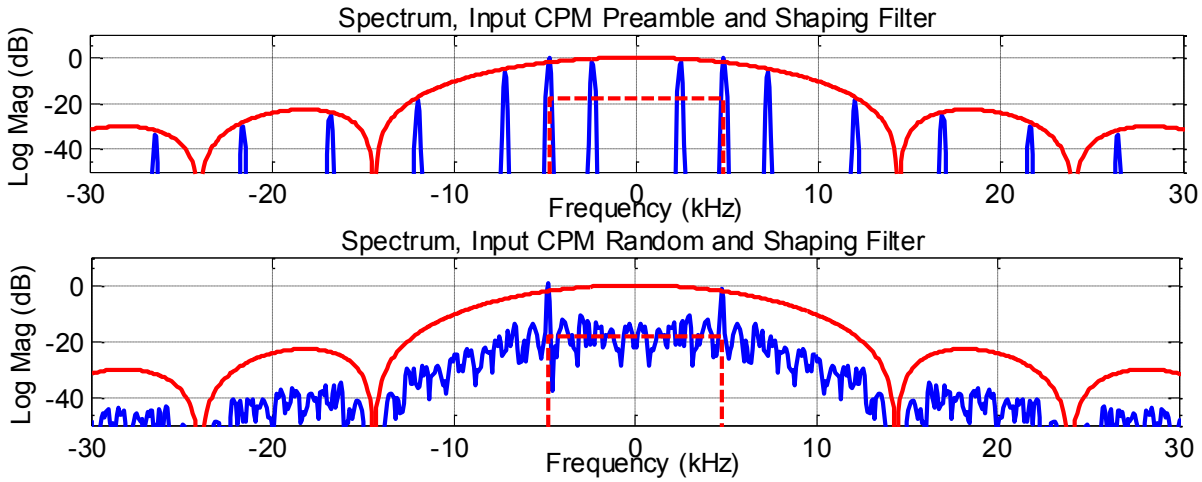

Figure 7. Upper Subplot: Spectra of Periodic Preamble and of Shaping Filter
Lower Subplot: Spectra of Random CPM Data and Shaping Filter.

III. OPTIMUM RECEIVER FOR CPM SIGNALS

The waveform used by the radio is the conventional continuous phase modulation formed by linear phase transitions around the unit circle in the positive and negative directions for logical 0's and 1's respectively. Demodulation of this signal can be performed by an O QPSK down conversion as is done in most CPM receivers. Here we form matched filters for the I and Q components separately as the sum of products with the two weight sets cos(θ n) and –sin(θ n). The CPM phase matched filter forms the sum of products of the conjugate phase trajectory exp(j (θ n). Contrary to first impression, these are not the same. Figure 8 shows the I and Q components formed by the two processes. The O-QPSK peak I and Q components are orthogonal with magnitude 10 sqrt(2) while the CPM peak I component is 20. The noise component responses of the complex O-QPSK and real CPM signal are the same at 3.16.The output SNR of the two options are 13 dB and 16 dB respectively. Two effects are at play here; the real CPM matched filter forms x·c + y·s as opposed to x·c + j·y·s and the CPM filter also rejects half the noise of the O-QPSK process. An interesting property of the CPM process is that the imaginary part forms the derivative matched filter which the O-QPSK system must also form in two additional filters to support its timing recovery loop. We have observed the same property of other shaped CPM signal sets in the MIL-STD-188.

There are two phase profiles, CW and CCW, in the binary CPM signal set. Thus there must be two matched filters one for each profile. Both filters must operate in each symbol interval and their outputs must be examined. Each filter can have a positive or a negative local maxima and the filter with the largest output is selected as the proper filter for the spin direction for that interval and hence identifies the logic level carried by that symbol interval. The top subplot of fig. 9 shows the time signal at the start of the preamble. Here we removed the Doppler offset to clearly show the matched filter responses. The two center subplots show the matched filter responses to the preamble sequence. Here we see the 2 responses to the 1 1 sequence in MF_1 and then the 2 responses to the 0 0 sequence in MF_0. The blue and red curves are the real and imaginary parts of the filter responses. Note that at the extrema points of each blue curve, the red curve goes through its' zero crossings, hence is (within a sign change) the derivative matched filter response.

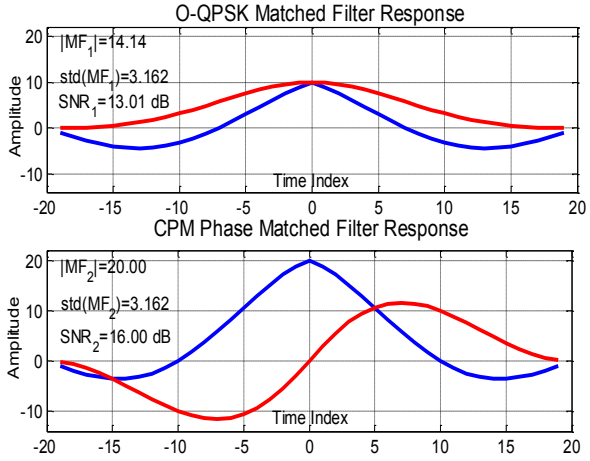

Figure 8 Matched Filter Response, OQPSK and CPM Process.

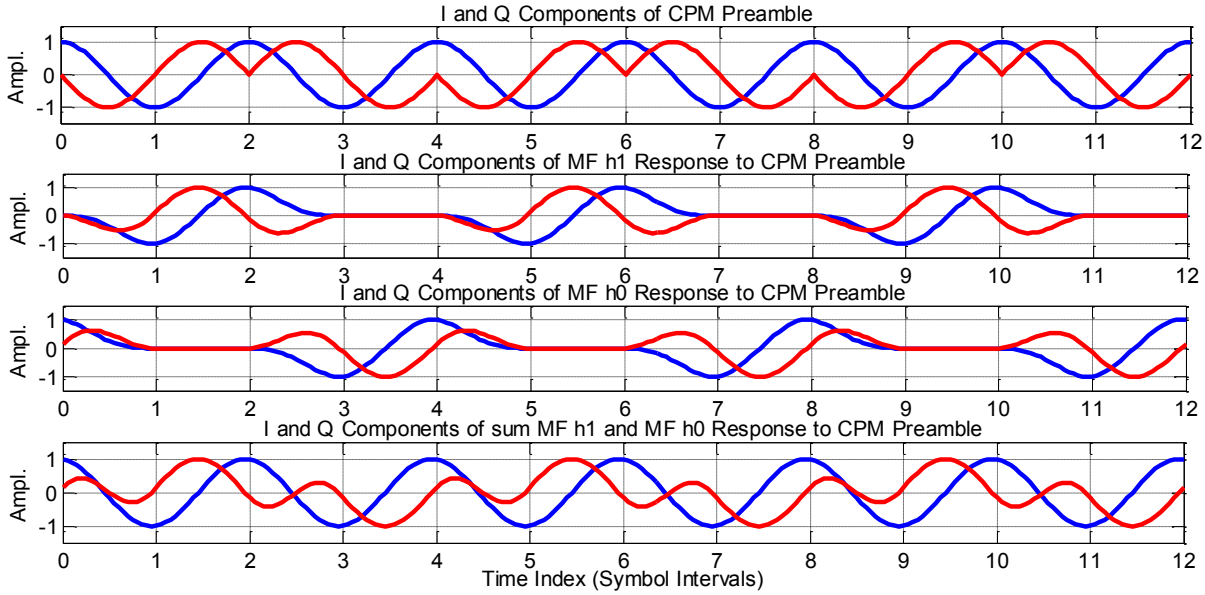

Figure 9. I & Q Input Signal and Two Matched Filter and the Sum of I & Q Responses of CPM Preamble Process.

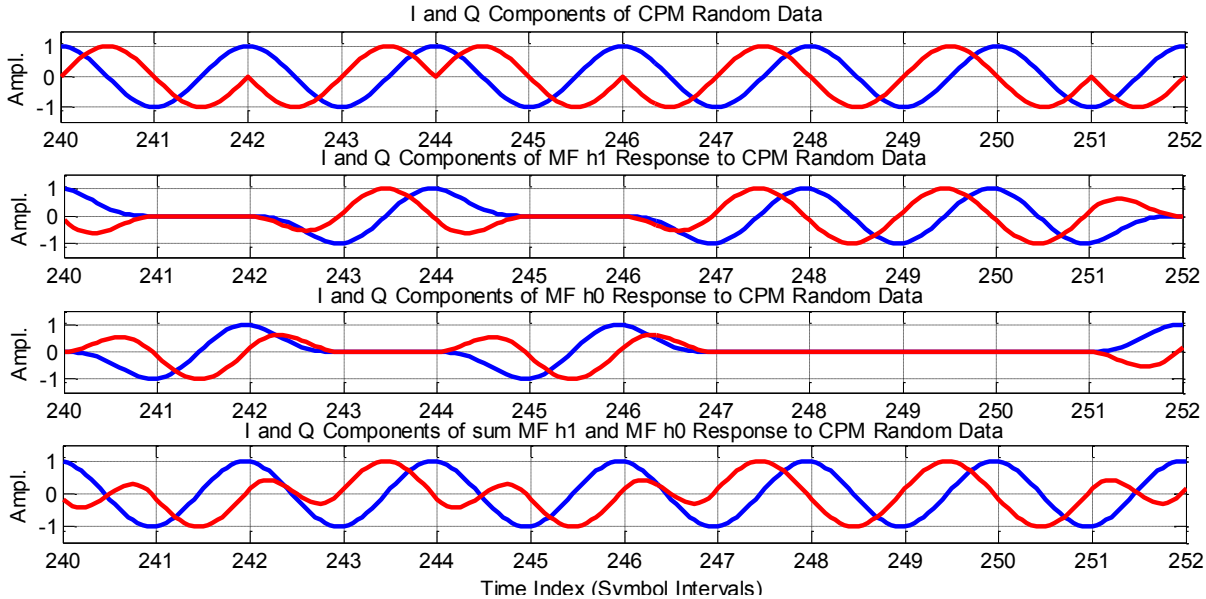

Figure 10. I & Q Input Signal, Two Matched Filters, and the Sum of I & Q Responses of CPM Random Data Process.

Note also in the two center subplots that at time tag 1 and 2 the matched filter h1 response peaks at -1 and +1 while the matched filter h0 response is 0 and 0. Then in the next interval time tags 3 and 4 the matched filter h1 response is 0 and 0 while the matched filter h0 response is -1 and +1. The responses of the 2 matched filters for CCW and CW rotation are seen to be orthogonal. This pattern repeats for the full preamble. What is remarkable is the sum of the matched filter response shown in the bottom subplot. The real part of the response is a cosine! Compare this response to the real part of the input signal in the top subplot. The detection process simply locates the location and value of the local extrema and then asks which of the two matched filter outputs is responsible for this extrema value?

The top subplot of fig. 10 shows the time signal at in the random data segment of the PCM time series. In practice, the Doppler offset had been removed by the Doppler processing the Doppler suppression in the preamble segment of the CPM signal. The two center subplots show the matched filter responses to the random data sequence. Here we see the responses to the 1 sequence in MF_1 and then the response to the 0 sequence in MF_0. The blue and red curves are the real and imaginary parts of the filter responses. We note that here too, at the extrema points of each blue curve, the red curve

goes through its' zero crossings, hence is (within a sign change) the derivative matched filter response. Note also in the two center subplots that at time tag 241 and 242 the matched filter h0 response peaks at -1 and +1 while the matched filter h1 response is 0 and 0. Then in the next interval time tags 243 and 244 the matched filter h1 response is -1 and 1 while the matched filter h1 response is 0 and 0 The responses of the 2 matched filters for CCW and CW rotation are seen to be orthogonal for both the preamble and the random data sequences. What continues to be remarkable is the sum of the matched filter response shown in the bottom subplot. The real part of the response is a cosine! Again we should compare this response to the real part of the input signal in the top subplot. The detection process simply locates the location and value of the local extrema and then asks which of the two matched filter outputs is responsible for this extrema value? The sample values at symbol time of each filter can assume one of three values, +1, 0, and -1 and if one filter has value +1 or -1, the other will have value 0.Once the correct filter has been identified the y-y_{dot} product moves the sample index to

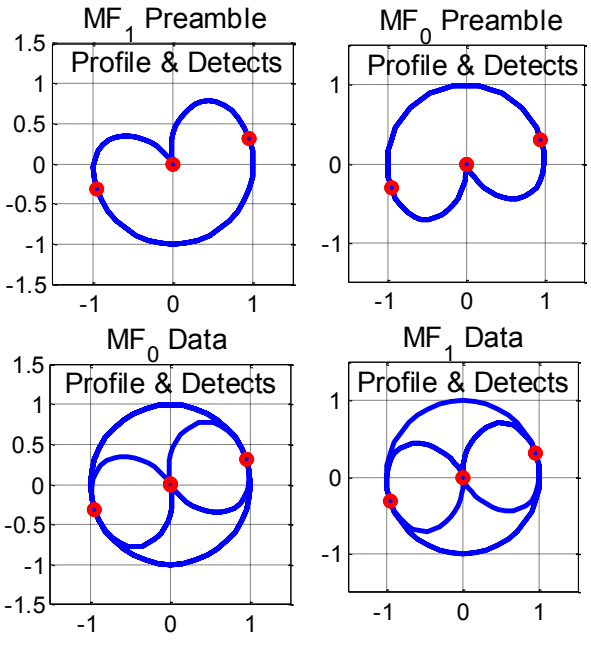

Figure 11. Phase Profiles and Detection Points for two Matched Filters in Preamble and Data Intervals.

the sample corresponding to the matched filter peak response. Once the peak sample position is identified, the phase angle of that index is used to control the phase PLL. Additional comment is presented in the following material.

Figure 11 shows the phase trajectories of the two matched filters along with the peak MF detection phase points on the profiles. Here we intentionally phase shifted the signal so that the detection points are off the horizontal axis. In this figure, the phase angle of the detection point supplies the angle errors for the phase PLL. The phase error seen here is typical of the residual phase after suppression of the frequency offset due to Doppler.

IV. CONCLUSIONS

We have presented in this paper a new approach to estimating and removing large Doppler frequency offsets for a Binary CPM Modulated signal. We then demonstrated the 3-dB SNR advantage of a phase profile matched filter based receiver compared to the more traditional O-QPSK approach to demodulating CPM signals. Finally we described and demonstrated some of the signal structures unique to the phase match matched filters with the filters offering detection information in their separate response while their sum provides the information for the timing recovery process.

V. ACKNOWLEDGEMENT

The Doppler estimation and removal process presented here was develop by the harris under a SPAWAR Contract to SDSU Foundation, contract No. N66001-15-D0099, "Tactical Secure Voice SDR Support (FY16)". SDSU is pursuing a patent based on the Doppler estimation process. The design and implementation of the modem using the Doppler estimation and the phase profile matched filters was an extension of this work started in 2016 and completed by the authors while harris was a SPAWAR 2017 ONR Summer fellow.

REFERENCES

[1] Pierre E Laurent, "Exact and Approximate Construction of Digital Phase Modulators by Superposition of Amplitude Modulated Pulses (AMP)", IEEE Trans. On Comm. VOL. Com-34, NO 2, Feb. 1986, pp. 150-160.

[2] Marvin. K Simon, "Carrier Synchronization of Offset Quadrature Phase-Shift Keying", Jet Propulsions Laboratory, California Institute of Technology, Telecommunications and Mission Operations (TMO) Progress Report TMO PR 42-133 Jan-Mar, 1998.

[3] Arjun Ramamurthy, fredric j. harris, "An All-Digital Implementation of Constant Envelope-Bandwidth efficient GMSK Modem using Advanced Digital Signal Processing Techniques", Wireless Personal Communications, Jan. 2010, VOL. 52, Issue 1, pp 133-146.

[4] Mohamed K. Nezami, "Techniques for Acquiring and Tracking MIL-STD-181B Signals", MILCOM-2002 Proceedings, Anaheim CA, 25-Feb. 2003, pp. 224-231.

[5] Earl McCune, "Practical Digital Wireless Signals", Cambridge University Press. March 2010, ISBN 10-0521516307, Chapter 6, Phase Modulation, Section 6.1, Author's Dilemma.